Journal of Radioanalytical and Nuclear Chemistry (2022) 331:119–128
https://doi.org/10.1007/s10967-021-08064-5

Estimation of the natural radioactivity levels in the soil along the Little Zab River, Kurdistan Region in Iraq

Jahfer M. Smail[1] · Saddon T. Ahmad[2] · Habeeb Hanna Mansour[3]

Received: 26 June 2021 / Accepted: 11 October 2021 / Published online: 20 October 2021

Abstract
Gamma-ray spectrometry with high-purity germanium (HPGe) detector was used to estimate the natural radioactivity levels in the soil along the Little Zab River in the Kurdistan Region of Iraq. Results showed that the activity concentrations of ^{226}Ra, ^{232}Th, ^{40}K and ^{137}Cs were in ranges of 4.4–34.7, 1.5–13.3, 42.1–583.9 and 0.5–31.5 Bq kg^{-1}, respectively. Ra equivalent activities, absorbed dose rate and hazard indices in the study area were calculated and compared with the global average activity of the soil. The Ra equivalent activities of the studied samples were below the internationally accepted values and did not pose any health hazard to the population.

Keywords Radioactivity · Soil · Geological formation · Hazard · HPGe spectrometer

Introduction

Humans have been continuously exposed to natural radiation since the Earth's formation. The soil is the major source of radioactive nuclides in other materials, such as water, air, sediments and biological systems.[1] The levels of radiation are not the same in different parts of the world and depend on the concentration of radionuclides in the Earth's crust. The study of naturally occurring radioactive nuclides and their significance in organisms is gaining popularity [2].

Natural concentrations of radionuclides in the soil are usually associated with the concentration of these atoms in the substratum [3]. The levels of natural radioactivity in the soil have attracted attention, because all populations around the globe are exposed to natural radioactivity, depending on the concentration of these radionuclides. A significant component of the background radiation is produced by natural radionuclides in the soil [4].

Natural radioactive materials have also become of great interest in the publications and reports of the International Atomic Energy Agency issued by the European Council Directive [3]. Knowledge of the radionuclide distribution is important, because it provides useful information for the observation of the natural environmental radioactivity and associated external exposure resulting from primary gamma radiation based on geological and geographical conditions. Such radiation can be observed at varied levels in the rocks in the different regions worldwide. The concentrations of the natural radionuclides ^{238}U, ^{232}Th and their daughters, as well as ^{40}K, in the soil and rocks depend on the local geology and causes a diversity of dosages [5, 6]. This study was performed to identify the concentrations of the activities of ^{226}Ra, ^{232}Th, ^{40}K and ^{137}Cs in the soil samples along the Little Zab River Basin (LZRB) in Iraq and to assess their radiological impact in the region.

Materials and methods

Study area

The present study was carried out in several regions from the north to the south of the Little Zab River (LZR) in the Kurdistan Region of Iraq. The study area extends from 35°47′23.3" N to 36°11′28.4" N and from 44°10′26.3" E

✉ Jahfer M. Smail
jahfer.majeed@koyauniversity.org

[1] Department of Physics, Faculty of Sciences and Health, Koya University, Koya KOY45, Kurdistan Region, Iraq

[2] School of Medicine, Koya University, Koya KOY45, Kurdistan Region, Iraq

[3] Department of Physics, College of Education, Salahaddin University, Hawler, Iraq

to 45°15′43.6" E and covers ~ 5,635 km^2. The geographical position of the sampling locations is shown in Fig. 1.

The LZR, which is also known as the Lower Zab or Lesser Zab River, is the largest tributary of the Tigris River with ~ 71% of its basin situated in Iraq and the rest in Iran. The total length of the river is 456 km. It enters from Iran in the northeast of Iraq, follows many anticlines and meanders around the plunges, until it flows out of the mountainous area [7]. The average annual flow of water to the river reaches 7.17 km^3, whilst its 5.07 km^3 is being retarded by the Dukan Dam, which was built on the river path. Thus, the LZR is considered to be the main source for the annual filling of the dam. As the river flows into Iraq, it encounters several different geological structures, the ages of which go back to the Jurassic to Quaternary periods. For example, the upper part of the river is located within the Zagros suture zone, whereas its lower part is within the foothills with clastic unresisting rocks [8, 9].

Sample collection

Thirteen separate geological formations (laid at 23 sites) along the LZR were selected for the collection of soil samples to determine the activity concentration of naturally occurring radionuclides in the soil. Figure 1 illustrates the geographical positions of the sampling sites. A core method, with a core diameter of 15 cm and a depth of 20 cm, was used to collect the soil samples [10, 11]. Soil depth was considered to be particularly significant in areas with highly inhomogeneous distribution of radionuclides. After the stones and inorganic materials were removed, the soil samples were dried in an electric oven at approximately 105 °C, crushed and sieved through a 2 mm mesh sieve [12, 13]. For the gamma spectrometry device, 1 kg of each sample was packed in a 1 L Marinelli beaker, and the beaker was closed for 4 weeks to create a secular equilibrium between the Ra content of the samples and the radionuclides of its daughter [14, 15].

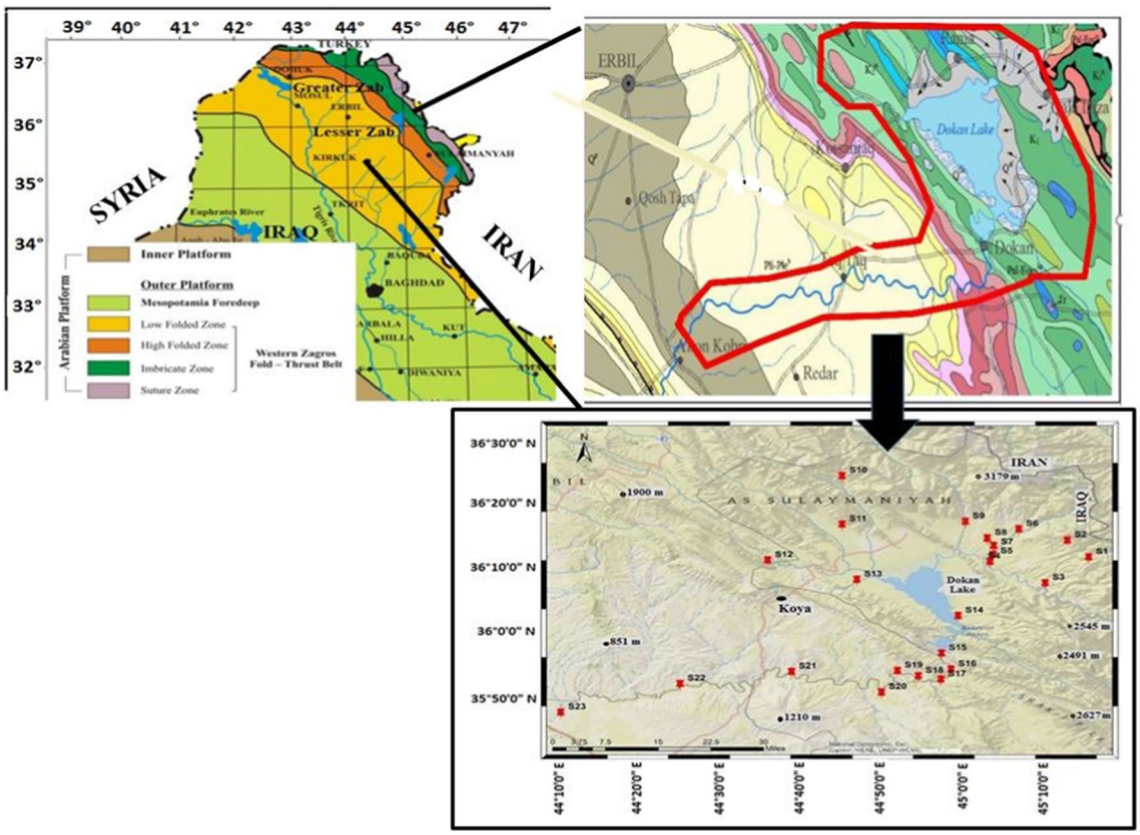

Fig. 1 Map of the study area and sampling sites

Counting of samples

The multichannel analyser and a high-purity germanium (HPGe) gamma-ray spectrometry system were used to count the gamma rays emitted from the soil samples. The activity concentrations of the radionuclides in the soil samples were determined by using a counting system made by Princeton Gamma Tech at Koya University. The HPGe coaxial detector had a relative efficiency of 73%, a peak-to-Compton ratio of 75/1 and crystal size with an active volume of 265 cm^3. To secure the measurement station from the background radioactivity, the detector was placed in a lead well with a thickness of 10 cm.

The system was optimised for energy and resolution calibration by using three common sources, namely, ^{60}Co, ^{137}Cs and ^{226}Ra. Efficiency calibration was achieved by following the same approach as that demonstrated by Ahmad [16] and Ahmad et al. [17]. The samples were put over the detector for at least 10 h. An empty beaker was counted within a 10-h measurement period to assess the background radiation in the detector location. The net peak region of gamma rays of the measured isotopes was corrected using the background spectra. After background calculation and subtraction, the naturally occurring radionuclides ^{226}Ra, ^{232}Th and ^{40}K appeared in the new spectrum of the measured gamma ray [15].

The activity concentration of ^{226}Ra was estimated using the gamma-ray lines of 351.9 keV (35.8%) gamma rays from the ^{214}Pb decay and 609.3 keV (44.8%) and 1764.5 keV (15.36%) gamma rays from the ^{214}Bi decay. The weighted average of the activity calculated using the gamma-ray lines of 238.6 keV (43%) from the ^{212}Pb decay and 583 keV (84.5%) and 2614.5 keV (99.16%) from the ^{208}Tl decay were used to calculate the activity concentration of ^{232}Th. In addition, 1460.8 keV (10.7%) gamma-ray line was used to assess the activity concentration of ^{40}K [18, 19]. ^{137}Cs was also directly determined using the 661.7 keV (85.21%) gamma-rays line.

Calculations

Activity concentration

The activity concentration ($\boldsymbol{A}$) of ^{226}Ra, ^{232}Th, ^{40}K and ^{137}Cs in the soil samples were calculated as follows [20–22]:

$$A = \left(\frac{N}{\varepsilon I_\gamma TM}\right) \tag{1}$$

where N is the net count, ε is the absolute gamma peak efficiency of the detector of this particular gamma-ray energy, I_γ is the decay intensity of the specific energy peak (including the decay branching ratio), T is the counting time of the measurement in seconds, M is the mass of the sample in kilogram. The relative combined standard deviation σ_A of the activity concentration is given by the formula [23]:

$$\frac{\sigma_A}{A} = \sqrt{\frac{\sigma_N^2}{N} + \frac{\sigma_\varepsilon^2}{\varepsilon} + \frac{\sigma_{I_\gamma}^2}{I_\gamma} + \frac{\sigma_M^2}{M}} \tag{2}$$

where σ_N is the standard deviation of the N net count rate per second, σ_ε, σ_{I_γ} and σ_M are the standard deviations of the ε, I_γ and M, respectively.

Efficiency calibration of the HPGe detector

The efficiency was calibrated by using the three standard gamma ray sources of ^{226}Ra, ^{60}Co and ^{137}Cs. These samples were placed over the detector for at least 1 h. The spectra were evaluated by using a Thermo Scientific multi-channel analyser and the Princeton Gamma Tech computer software program QuantumGold 2001.

The measured data were well fitted by the *RJS Graph 3.93.01* software to obtain the following power equation:

$$\varepsilon = 8.5758 \times E_\gamma^{-0.896} \tag{3}$$

where ε is the absolute full peak efficiency of the detector, and E_γ is the energy of the gamma ray. Figure 2 shows the plotted graph of the absolute full peak efficiency and gamma-ray energy (Table 1).

Radium equivalent activity (Ra_{eq})

The distribution of natural radionuclides in soils is not uniform. Therefore, the total exposure to radiation from ^{226}Ra, ^{232}Th and ^{40}K nuclides was expressed by the Ra_{eq}) in (Bq

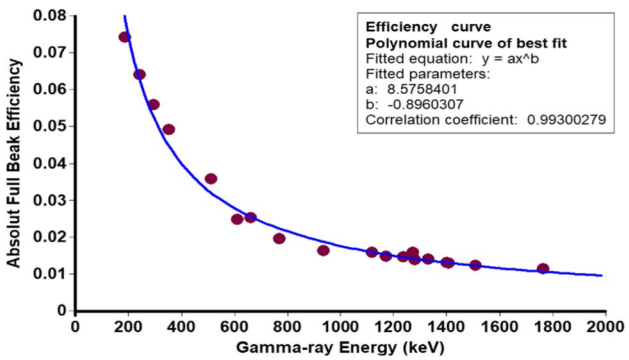

Fig. 2 Absolute full peak efficiency against the gamma-ray energy of the HPGe detector

Table 1 Code of samples based on the soil geological formation

Code of samples	Location	Geographical coordinate		Geological formation
		Latitude	Longitude	
S1	Halsho	36°11′28.4" N	45°15′43.6" E	Shiranish Formation (Late Campanian–Maastrichtian)
S2	Shexawdalan	36°13′18.0" N	45°13′58.2" E	Shiranish Formation (Late Campanian–Maastrichtian)
S3	Kawya	36°07′27.0" N	45°10′20.0" E	Qamchuqa Formation (Hauterivian-Albion)
S4	Sndolan	36°10′45.6" N	45°03′18.4" E	Quaternary sediment Alluvial Formation
S5	Braymawa	36°11′53.5" N	45°03′54.1" E	Quaternary sediment Alluvial Formation
S6	Grdestr	36°15′47.7" N	45°07′04.4" E	Quaternary sediment Alluvial Formation
S7	Zharawa	36°13′41.2" N	45°04′21.3" E	Quaternary sediment Alluvial Formation
S8	Bastasten	36°14′23.8" N	45°03′11.5" E	Quaternary sediment Alluvial Formation
S9	Sangasar	36°16′42.4" N	44°57′07.0" E	Quaternary sediment Alluvial Formation
S10	Daraban	36°24′05.4" N	44°45′13.7" E	Sargalu Formation (Bajocian-Bathonian)
S11	Sawchawa	36°16′24.6" N	44°45′16.3" E	Tanjaro Shiranish Formation (Late Campanian- Maastrichtian)
S12	Jaly	36°11′00.4" N	44°36′04.3" E	Tanjaro Shiranish Formation (Late Campanian- Maastrichtian)
S13	Khdran	36°07′59.0" N	44°47′03.5" E	Tanjaro Shiranish Formation (Late Campanian- Maastrichtian)
S14	Tangzha	36°02′20.3" N	44°59′35.7" E	Quaternary sediment Dokan Conglomerate Formation
S15	Lower Dokan	35°56′30.0" N	44°57′30.7" E	Tanjaro Shiranish Formation (Late Campanian- Maastrichtian)
S16	Sartk	35°54′03.3" N	44°58′45.4" E	Tanjaro Shiranish Formation (Late Campanian- Maastrichtian)
S17	Dwawan	35°53′01.4" N	44°54′39.7" E	Sinjar and Kolosh Formation
S18	Klesa	35°52′56.0" N	44°54′47.7" E	Fatha Formation
S19	Bogd	35°53′47.4" N	44°52′05.4" E	Injana Formation
S20	Goptapa	35°50′26.6" N	44°50′06.9" E	Mukdadiya Formation
S21	Mokharas	35°53′42.5" N	44°38′57.4" E	Bai Hassan Formation
S22	Segrdkan	35°51′46.6" N	44°26′35.0" E	Bai Hassan Formation (Pliocene – Pleistocene)
S23	Prde	35°47′23.3" N	44°10′26.3" E	Quaternary sediment polygenetic Formation

kg^{-1}). The Ra_{eq} in the soil samples was calculated as follows [22, 24]:

$$Ra_{eq} = \left(A_{Ra}\right) + \left(1.43A_{Th}\right) + \left(0.077A_{K}\right) \quad (4)$$

where A_{Ra}, A_{Th} and A_K represent the activity concentrations of ^{226}Ra, ^{232}Th, and ^{40}K, respectively. According to the OECD of 1979 [25], the safe value of Ra_{eq} for any naturally occurring radioactive materials is less than 370 Bq kg^{-1}.

Absorbed gamma dose rates (D_Rs)

To determine the uniform distribution of the naturally occurring radionuclides, the absorbed gamma D_Rs in the air at 1 m above the ground surface were calculated based on the guidelines provided by UNSCEAR (2000) [21]:

$$D_R\left(nGy\,h^{-1}\right)(NORM) = (A_{Ra} \times 0.462) + (A_{Th} \times 0.604) + (A_K \times 0.0417) \quad (5)$$

Annual effective dose (AED)

The AED) was calculated from the absorbed gamma D_R by using the dose conversion factor of 0.7 Sv Gy^{-1} with an outdoor occupancy factor of 0.2 and 0.8 for indoor as given by UNSCEAR (2000) [21]. The AED was determined as follows:

$$AED\left(\mu Sv\,y^{-1}\right) = D_R\left(nGy\,h^{-1}\right) \times T \times F \quad (6)$$

where D_R is the calculated dose rate (nGy h^{-1}), T is the occupancy time and F is the conversion factor (0.7 Sv Gy^{-1} for environmental exposure to gamma rays of moderate energy as published in UNSCEAR 1993 [26] and UNSCEAR 2000). The outdoor occupancy factor T is approximately 20% of 8760 h y^{-1}. The outdoor annual effective dose equivalent was determined given as follows:

$$AED_{outdoor}\left(\mu Sv\,y^{-1}\right) = D_R\left(nGy\,h^{-1}\right) \times (0.2 \times 8760\,h\,y^{-1}) \times 0.7\left(Sv\,Gy^{-1}\right) \quad (7)$$

External hazard index (H_{ex})

The external hazard index was calculated by assuming that 370 Bq $kg^{-1}$of ^{226}Ra, 259 Bq kg^{-1} of ^{232}Th and 4810 Bq $kg^{-1}$of ^{40}K produce the same gamma dose rates. The following relation was used to evaluate the external hazard index [27, 28]:

$$H_{ex} = \left(A_{Th}/259\right) + \left(A_{Ra}/370\right) + \left(A_{Ra}/4810\right) \leq 1 \quad (8)$$

The external hazard index for ^{232}Th,^{226}Ra and ^{40}K, was less than 1 mSv y^{-1}, corresponding to the Ra_{eq} of 370 Bq kg^{-1} (OECD-1979) [25].

Result and discussion

Table 2 shows the activity concentrations of the natural radioactive nuclides ^{226}Ra, ^{232}Th and ^{40}K and the artificial radionuclide $^{137}C_S$ in the samples in the different geological formations along the LZR. The mean values (range) of the activity concentrations of ^{226}Ra, ^{232}Th, ^{40}K and $^{137}C_S$ in soils were 13.8 ± 0.5 (4.4–34.7), 6.5 ± 0.2 (1.5–13), 276.5 ± 4.4 (42–583) and 7.0 ± 0.2 (0.5–31.5) Bq kg^{-1}, respectively. The variations in the activity concentrations of the naturally occurring radionuclides in the soil depended on the geological and geographical conditions of the area.

For ^{226}Ra, the minimum activity concentration (4.4 ± 0.1 Bq kg^{-1}) was observed in the Tanjaro Shiranish Formation (S12), and the maximum value (34.7 ± 0.6 Bq kg^{-1}) was found in the Sargalu Formation (S10). For ^{232}Th, the maximum activity concentration (13.3 ± 0.2 Bq kg^{-1}) was found in the Quaternary sediment Dokan Conglomerate Formation (S14), and the minimum activity concentration (3.2 ± 0.1 Bq kg^{-1}) was observed in the Sinjar and Kolosh Formation (S17). For ^{40}K, the maximum activity concentration (583.9 ± 8.2 Bq kg^{-1}) was found in the Shiranish Formation (S2), and the minimum specific activity concentration (42.1 ± 0.9 Bq kg^{-1}) was found for the Tanjaro Shiranish Formation (S12). For $^{137}C_{S,}$ the maximum specific activity concentration (31.5 ± 0.3 Bq kg^{-1}) was found in the Mukdadiya Formation (S20), and the minimum activity concentration (0.5 ± 0.1 Bq kg^{-1}) for the sample Shiranish Formation (S1).

The activity concentrations of the ^{226}Ra, ^{232}Th and ^{40}K radionuclides were not consistent with each other and did not record similar patterns in the different samples. Thus, these radionuclides were random in terms of their minimum

Table 2 Activity concentrations of radionuclides in the soil samples

Code of samples	Location	Activity concentration (Bq Kg^{-1})			
		^{226}Ra	^{232}Th	^{40}K	^{137}Cs
S1	Halsho	10.7 ± 0.5	6.2 ± 0.2	254.4 ± 4.1	31.5 ± 0.3
S2	Shexawdalan	13.3 ± 0.6	8.6 ± 0.2	583.9 ± 8.2	13.8 ± 0.2
S3	Kawya	9.2 ± 0.4	4.9 ± 0.2	275.8 ± 4.4	1.4 ± 0.1
S4	Sndolan	15.8 ± 0.5	9.4 ± 0.2	431.4 ± 6.3	1.7 ± 0.1
S5	Braym Awa	18.3 ± 0.6	11.8 ± 0.3	442.9 ± 6.4	4.8 ± 0.2
S6	Grd Estr	21.2 ± 0.6	8.6 ± 0.2	388.2 ± 5.8	11.8 ± 0.2
S7	Zharawa	14.3 ± 0.5	6.4 ± 0.2	258.7 ± 4.2	5.6 ± 0.2
S8	Bastasten	22.6 ± 0.6	8.7 ± 0.2	325.4 ± 5	9.6 ± 0.2
S9	Sangasar	21.2 ± 0.6	8.5 ± 0.2	288 ± 4.5	8.3 ± 0.2
S10	Daraban	34.7 ± 0.6	5.4 ± 0.2	224.5 ± 3.8	17.8 ± 0.3
S11	Sawchawa	17.9 ± 0.5	10.3 ± 0.2	320.6 ± 4.8	4 ± 0.2
S12	Jaly	4.4 ± 0.1	1.7 ± 0.1	42.1 ± 0.9	0.7 ± 0
S13	Khdran	11.6 ± 0.4	5.3 ± 0.2	180.4 ± 3.1	9.2 ± 0.2
S14	Tanzha	11.8 ± 0.4	13.3 ± 0.2	237.2 ± 4	14 ± 0.2
S15	Lower Dokan	10.3 ± 0.4	4.8 ± 0.2	224.7 ± 3.7	3.2 ± 0.1
S16	Sartk	7.9 ± 0.4	3.2 ± 0.1	155.4 ± 2.9	4.1 ± 0.1
S17	Dwawan	5.2 ± 0.3	1.5 ± 0.1	73.4 ± 1.6	0.7 ± 0.1
S18	Klesa	11.3 ± 0.5	5.8 ± 0.2	299.6 ± 4.6	6.6 ± 0.2
S19	Bogd	10.4 ± 0.4	4.2 ± 0.1	217.6 ± 3.5	4.7 ± 0.2
S20	Goptapa	9.4 ± 0.4	5.2 ± 0.1	248.9 ± 4	0.5 ± 0.1
S21	Mokharas	10.3 ± 0.5	4.7 ± 0.2	274.3 ± 4.3	1.3 ± 0.1
S22	Segrdkan	11.8 ± 0.5	5.8 ± 0.2	293 ± 5	2.4 ± 0.1
S23	Prde	13.5 ± 0.4	6 ± 0.2	318.1 ± 4.9	2.5 ± 0.2
Average		13.8 ± 0.5	6.5 ± 0.2	276.5 ± 4.4	7 ± 0.2

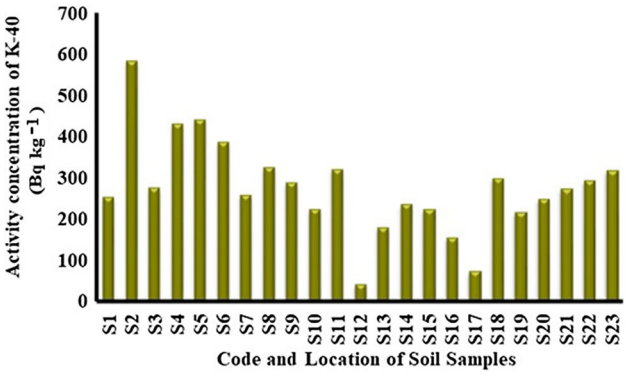

Fig. 3 Activity concentration of ^{40}K in the soil samples

Table 3 Comparison of the ranges of activity concentrations of the naturally occurring radionuclides in the study area with those from similar investigations in other countries

Country	Activity concentration of NORM in virgin soil (Bq kg^{-1})			References
	^{226}Ra	^{232}Th	^{40}K	
Algeria	47	33	329	[33]
Turkey	13–31	12–37	285–614	[34]
Iran	20	23	613	[35]
Qatar	22.5	7.7	165.8	[36]
China	9–145	15–102	417–1263	[32]
Malaysia	45–111	52–127	99–173	[31]
India	3–16	37–299	338–544	[37]
Iraq	16–39	9–28	262–613	[30]
Iraq	4.4–34.7	1.5–13.3	42–584	Present study
Median in worldwide	16–110	11–64	140–850	[21]
Worldwide Average	35	30	400	[21]

and maximum values, but they are still generally within the limits of low and moderate levels of radioactivity. The fluctuations may be due to the topography of the region, which has hills and valleys.

The mountainous topography may allow the movement or the accumulation of radionuclide with the rainwater flow because of the ability of the chemical compounds to dissolve or undergo sedimentation and stagnation. Such assumptions could also be used to explain the ^{137}Cs distribution by further assuming that the ^{137}Cs was not naturally distributed. This compound may originally have a constant level as a fallout but became disturbed by environmental conditions and slightly accumulated in depressions and ponds.

Figure 3 shows the activity concentration of ^{40}K in the soil samples. The obtained values were within the global average values [29]. The activity concentrations of the samples from the study area were compared with those from similar investigations in other countries (Table 3). The range of the activity concentrations of ^{226}Ra was consistent with the results from Nineveh Province obtained by Najam et al. [30]. and most of other studies in different countries but lower than the results from Malaysia [31] and China [32]. The range of the activity concentrations of ^{232}Th was in the level of the results from the Nineveh Province [30] and almost lower than those of all other studies. The ^{40}K results were comparable with the results from other studies as shown in Table 3 and matched the world average. However, the maximum level of ^{40}K in China [32] was almost twice the level in this study.

To compare the activity concentrations of ^{232}Th, ^{226}Ra and ^{40}K in the soil samples, the Ra_{eq} as a common index was used to obtain the sum of activities and estimate the radiological hazards, external H_{ex}, external D_R and outdoor AED for the virgin soil samples in this study (Table 4).

The calculated value of Ra_{eq} in the virgin soil samples varied in the range of 10–70.6 Bq kg^{-1}, with the average value of 44.4 Bq kg^{-1}. Variations in the Ra_{eq} values in the different soil samples depended on the type and content of the natural radionuclide. Figure 4 shows that the Ra_{eq} in the soil sample was lower than the global average value. The obtained Ra_{eq} values in the soil samples were within the recommended limit of 370 Bq kg^{-1}.

Absorbed gamma D_Rs were found to be in the range of 4.9–37.2 nGy h^{-1}, with an average value of 22.6 nGy h^{-1}. The estimated average value of the absorbed gamma D_Rs was lower than the worldwide average value of 59 nGy h^{-1} as reported by UNSCEAR 2000 [21]. The measured value of the outdoor AED was in the range of 5.97–45.65 Sv y^{-1}, with an average value of 27.7 Sv y^{-1}. As illustrated in Fig. 5, the calculated values of the absorbed gamma D_Rs and annual effective dose equivalent for the virgin soil samples were also lower than the global average value.

The external H_{ex} was found to be in range of 0.02–0.18 mSv y^{-1}. The external H_{ex} values for the soil samples in the study area were lower than the recommended standard of 1 mSv y^{-1} by OECD in 1979 [25].

Intercomparison of the activity levels of the radionuclides in the sampled locations

The activity levels of the ^{226}Ra, ^{232}Th and ^{137}Cs (Fig. 5a) and ^{40}K (Fig. 5b) were compared using the average values from four groups of samples. These groups were divided according to the administrative division of the region. The subregions were Pshdar, Betwen, Lower Dokan and Taq Taq. Pshdar generally had the highest level of activity for the four radionuclides, whilst Lower Dokan showed the lowest levels for ^{226}Ra, ^{232}Th and ^{40}K. The radioactivity level of ^{137}Cs in Pshdar was more than four times its level in Taq Taq.

Table 4 External absorbed gamma dose rates (D_R), External hazard index (H_{ex}), Outdoor annual effective dose (AED) and Radium equivalent activity (Ra_{eq}) for soils

Code of samples	Location	Ra_{eq} (Bq kg^{-1})	D_R out (nGy h^{-1})	AED (μSv y^{-1})	H_{ex}
S1	Halsho	39.2 ± 1	22.8 ± 0.5	28 ± 0.6	0.106 ± 0.003
S2	Shex Awdalan	70.6 ± 1.5	37.2 ± 0.8	45.65 ± 0.93	0.191 ± 0.004
S3	Kawya	37.5 ± 1	18.9 ± 0.5	23.15 ± 0.59	0.101 ± 0.003
S4	Sndolan	62.4 ± 1.3	31.2 ± 0.7	38.19 ± 0.8	0.169 ± 0.004
S5	Braym Awa	69.2 ± 1.5	34.6 ± 0.7	42.38 ± 0.91	0.187 ± 0.004
S6	Grd Estr	63.3 ± 1.3	32.5 ± 0.7	39.81 ± 0.8	0.171 ± 0.004
S7	Zharawa	43.4 ± 1	21.9 ± 0.5	26.87 ± 0.63	0.117 ± 0.003
S8	Bastasten	60.1 ± 1.3	30.4 ± 0.7	37.22 ± 0.81	0.162 ± 0.004
S9	Sangasar	55.5 ± 1.2	27.9 ± 0.6	34.16 ± 0.72	0.15 ± 0.003
S10	Daraban	59.8 ± 1.1	30.7 ± 0.6	37.61 ± 0.68	0.161 ± 0.003
S11	Sawchawa	57.2 ± 1.2	28.3 ± 0.6	34.65 ± 0.71	0.155 ± 0.003
S12	Jaly	10 ± 0.3	4.9 ± 0.1	5.97 ± 0.16	0.027 ± 0.001
S13	Khdran	33.1 ± 0.9	17.1 ± 0.5	21 ± 0.57	0.089 ± 0.003
S14	Tanzha	49.1 ± 1	25 ± 0.5	30.61 ± 0.62	0.133 ± 0.003
S15	LowerDokan	34.5 ± 0.9	17.4 ± 0.5	21.32 ± 0.56	0.093 ± 0.003
S16	Samane Mase	24.4 ± 0.8	12.5 ± 0.4	15.33 ± 0.49	0.066 ± 0.002
S17	Dwawan	13.1 ± 0.6	6.5 ± 0.3	7.93 ± 0.36	0.035 ± 0.002
S18	Klesa	42.7 ± 1.1	22 ± 0.5	26.92 ± 0.66	0.115 ± 0.003
S19	Bogd	33.2 ± 0.9	17 ± 0.4	20.8 ± 0.53	0.09 ± 0.002
S20	Goptapa	35.9 ± 0.9	17.9 ± 0.5	21.92 ± 0.56	0.097 ± 0.003
S21	Mokharas	38.1 ± 1	19.2 ± 0.5	23.51 ± 0.62	0.103 ± 0.003
S22	Segrdkan	42.6 ± 1.1	21.4 ± 0.6	26.27 ± 0.68	0.115 ± 0.003
S23	Prde	46.7 ± 1.1	23.5 ± 0.5	28.76 ± 0.65	0.126 ± 0.003
Average		44.4 ± 1.1	22.6 ± 0.5	27.7 ± 0.6	0.120 ± 0.003
Worldwide average value		370	59	70	1

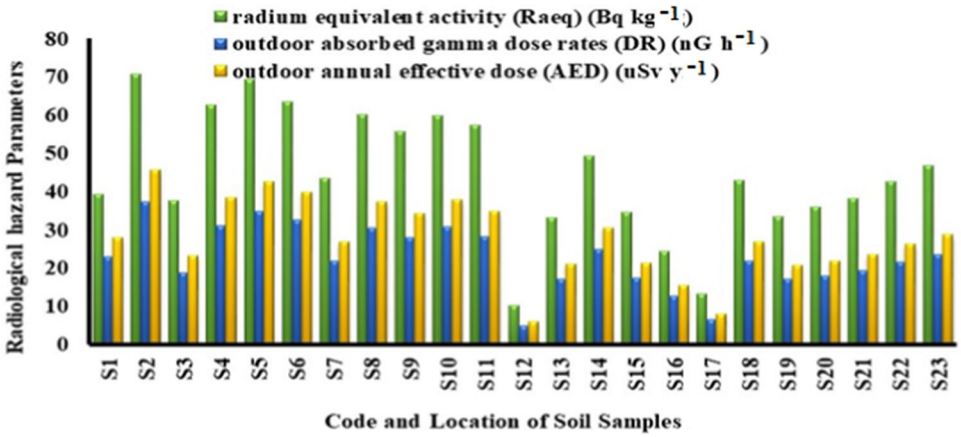

Fig. 4 External absorbed gamma dose rates (DR), radium equivalent activity (Ra_{eq}) and outdoor annual effective dose (AED) for the soil samples in the study area

Pshdar and Taq Taq showed higher levels of ^{40}K activity than the other two regions. The diversity in ^{137}Cs activity could be explained by considering the following: the level of the regions above sea level; the direction of the slope of region, where the eastern side is expected to receive a higher level of the ^{137}Cs fallout than the western side; and whether the region is stagnant, which keeps the accumulated ^{137}Cs,

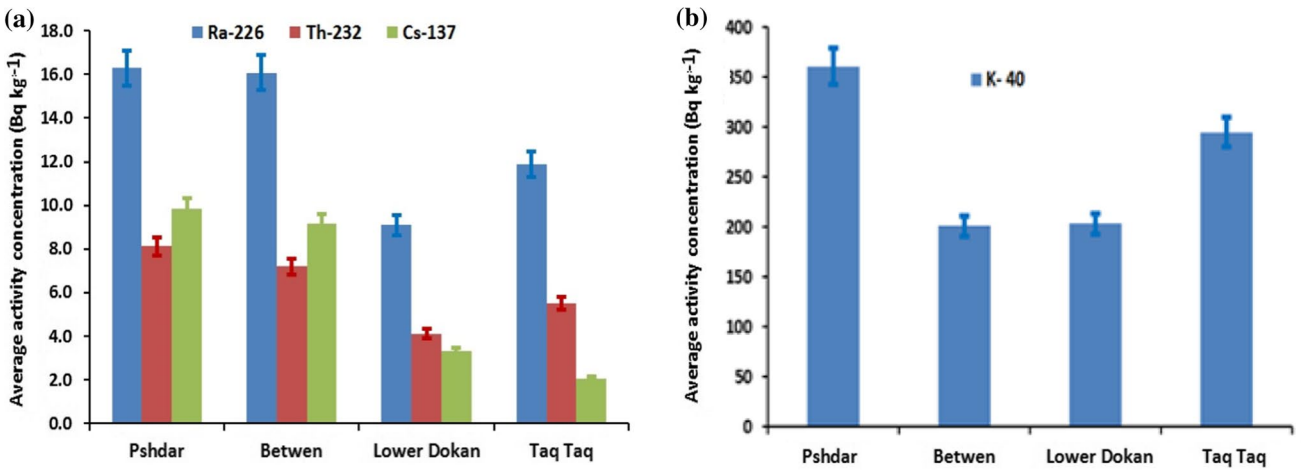

Fig. 5 Intercomparison of the average activities of **a** ^{226}Ra, ^{232}Th and ^{137}Cs and **b** ^{40}K in the four regions of the study area, with the weighted average of errors of each region

or a sloping area, which loses ^{137}Cs by being washed away by rainwater.

Histograms of the normality distribution of the primordial radionuclides

A histogram can be used to evaluate visually whether the data have symmetrical, normal, or Gaussian distribution or whether the distribution is asymmetrical or skewed. When the distribution is not normal, it cannot be accurately described by mean and standard deviation, but the median, quartiles and percentiles should be used. Figure 6 shows the frequency distributions of the primordial radionuclides (^{226}Ra, ^{232}Th and ^{40}K) and the man-made radionuclide (^{137}Cs). Figures 6a, b and c correspond to the distributions of ^{226}Ra, ^{232}Th and ^{40}K. The curves show that the three radionuclides had asymmetric distributions about the mean values, with positive skewness. The asymmetric tail were extending toward values that were higher than the mean values. Nevertheless, the distributions of these nuclei maintained a considerable normality. This result is in agreement with that of Sivakumar et al. [38]. ^{137}Cs showed a large positive skewness, indicating that its distribution was

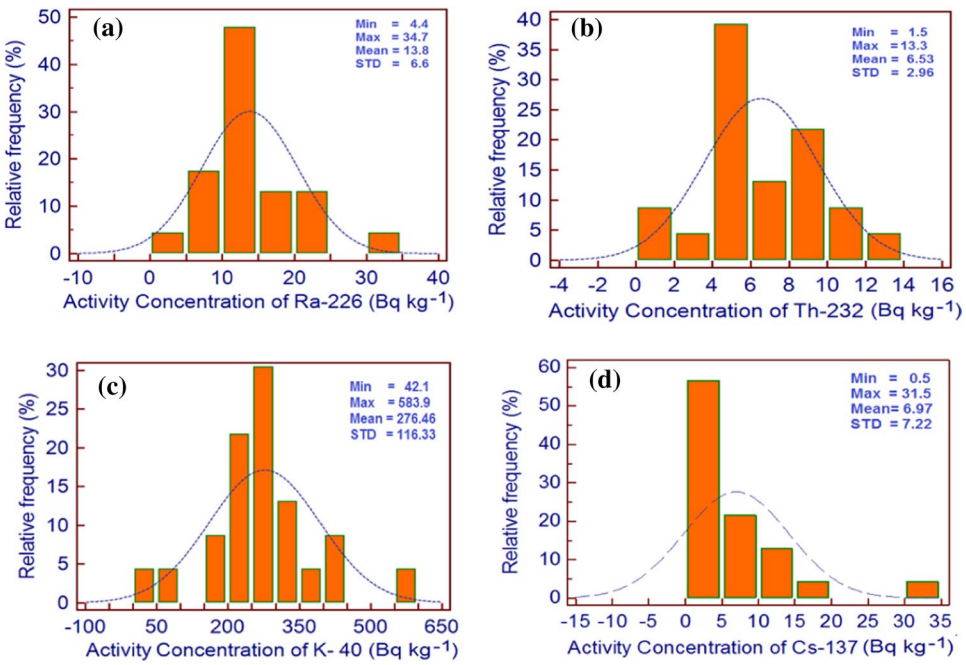

Fig. 6 Histograms of the activity concentrations of **a** ^{226}Ra, **b** ^{232}Th, **c** ^{40}K and **d** ^{137}Cs indicating the test for the normality of the distribution of these activities in the tested samples

asymmetric about the mean value, and the asymmetric tail was extending toward values that were higher than the mean value to a certain extent. This phenomenon rejects the normal distribution and removes the normality from this peak.

Conclusion

HPGe was used to measure the activity concentrations of ^{232}Th, ^{226}Ra,^{40}K and ^{137}Cs in the soil samples collected from the LZRB in Iraq. The mean values of the activity concentrations of ^{226}Ra, ^{232}Th, ^{40}K and ^{137}Cs varied in the ranges from 4.4 ± 0.1 to 34.7 ± 0.6, from 1.5 ± 0.1 to 13.3 ± 0.2, from 42.1 ± 0.9 to 583.9 ± 8.2 and from 0.5 ± 0.1 to 31.5 ± 0.3 Bq kg^{-1}, respectively. The measured radioactivity of the soil in the study area was below the worldwide average and posed no risk to the health of the population. Pshdar showed the highest level of radioactivity, whilst Taq Taq showed the lowest level. The regions that are more elevated above sea level had higher ^{137}Cs concentration than those areas at lower elevation above sea level.

Acknowledgements The authors would like to thank the Director of the Laboratory of Nuclear Radioactivity and the Director of the Centre for Scientific Research at Koya University for their support in the conduct of this study.

Declarations

Conflict of interest The authors declared that they have no conflict of interest.

References

1. Cengiz GB ÖEjcj (2002) Analysis of natural radioactivity levels in soil samples and dose assessment for Digor District, Kars, Turkey. Nat Ioniz Radiat Heal 1–175
2. Azeez HH, Mohammed MA, Abdullah GM (2021) Measurement of radon concentrations in rock samples from the Iraqi Kurdistan Region using passive and active methods. Arab J Geosci 14:572. https://doi.org/10.1007/s12517-021-06937-3
3. Azeez HH, Mansour HH, Ahmad ST (2020) Effect of using chemical fertilizers on natural radioactivity levels in agricultural soil in the Iraqi Kurdistan region. Polish J Environ Stud. https://doi.org/10.15244/pjoes/106032
4. Hussein ZA (2019) Assessment of Natural Radioactivity Levels and Radiation Hazards for Soil Samples Used in Erbil Governorate. Aro-the Sci J Koya Univ, Iraqi Kurdistan. https://doi.org/10.14500/aro.10471
5. Kadhim TM, Alkufi AA, Alhous SF (2020) Measurement of the natural radiological activity of soil samples of some general education schools in Al-Qadisiyah Governorate. IOP Conf Ser Mater Sci Eng. https://doi.org/10.1088/1757-899X/928/7/072026
6. Sadhukhan RK, Synzynys BI (2020) Natural radioactivity around Rooppur nuclear power plant before commissioning. J Phys Conf Ser 1701:012009. https://doi.org/10.1088/1742-6596/1701/1/012009
7. Sissakian VK, Fouad SF (2012) Geological map of Iraq, scale 1: 1000000. Iraq Geol Surv Publ Baghdad, Iraq
8. Sissakian V, Ahad AA, Al-Ansari N et al (2016) The regional geology of dokan area, NE Iraq. J Earth Sci Geotech Eng 6:35–63
9. Isamel J, Orhan H (2019) Palynofacies analysis of Naokelekan formation. Northern Iraq Oil Shale. https://doi.org/10.3176/oil.2019.2.05
10. Adhab HG, Kadhim SA, Alsabari EK (2020) Assessment excess lifetime cancer risk of soils samples in Maysan neighborhood adjacent to the middle Euphrates cancer center in Najaf / Iraq. IOP Conf Ser Mater Sci Eng. https://doi.org/10.1088/1757-899X/928/7/072100
11. Asaduzzaman K, Khandaker MU, Amin YM, et al (2014) Soil-to-root vegetable transfer factors for 226Ra, 232Th, 40K, and 88Y in Malaysia. J Environ Radioact 135:120–127
12. Tuo F, Peng X, Zeng Z et al (2021) Natural radionuclides distribution, depth profiles of caesium-137 and risk assessment for soil samples in west regions of China. J Radioanal Nucl Chem 327:831–838. https://doi.org/10.1007/s10967-020-07551-5
13. Khan IU, Sun W, Lewis E (2020) Estimation of various radiological parameters associated with radioactive contents emanating with fly ash from Sahiwal coal–fuelled power plant. Pakistan Environ Monit Assess 192:715. https://doi.org/10.1007/s10661-020-08669-5
14. Al-Alawy IT, Mhana WJ, Ebraheem RM (2020) Radiation hazards and transfer factors of radionuclides from soil to plant and cancer risk at Al-Taji city-Iraq. IOP Conf Ser Mater Sci Eng 928:072139. https://doi.org/10.1088/1757-899X/928/7/072139
15. Azeez HH, Ahmad ST, Mansour HH (2018) Assessment of radioactivity levels and radiological-hazard indices in plant fertilizers used in Iraqi Kurdistan Region. J Radioanal Nucl Chem 317:1273–1283. https://doi.org/10.1007/s10967-018-6001-3
16. Ahmad ST (2016) High purity Germanium Koya4039 Gamma detection system. ICEEAS-2016-Proceedings-Book 2016:268–276
17. Ahmad ST, Almuhsin IA, Hamad WM (2021) Radon activity concentrations in Jale and Mersaid warm water springs in Koya District, Kurdistan Region-Iraq. J Radioanal Nucl Chem 1–16
18. Gilmore GR (2011) Practical gamma-ray spectrometry. Wiley, Hoboken
19. Al-Alawy IT, Mhana WJ, Ebraheem RM et al (2020) Radiation hazards and transfer factors of radionuclides from soil to plant at Al-Tuwaitha City-Iraq. AIP Conf Proc 2290:50058. https://doi.org/10.1063/5.0027860
20. Bramki A, Ramdhane M, Benrachi F (2018) Natural radioelement concentrations in fertilizers and the soil of the Mila region of Algeria. J Rad Res Appl Sci 11(1):49–55
21. UNSCEAR (2000) Sources and Effects of Ionizing Radiation, United Nations Scientific Committee on the Effects of Atomic Radiation UNSCEAR 2000 Report to the General Assembly, with Scientific Annexes. United Nations Scientific Committee on the Effects of Atomic Radiation
22. Tran D-K, Truong Y, Le N-S et al (2020) Environmental radioactivity and associated radiological hazards in surface soils in Ho Chi Minh City. Vietnam J Radioanal Nucl Chem 326:1773–1783. https://doi.org/10.1007/s10967-020-07466-1
23. Currie L (2004) Quantifying uncertainty in nuclear analytical measurements, International atomic energy agency IAEA-TEC-DOC-1401 (Accessed October 8, 2021)
24. Hamza ZM, Kadhim SA, Hussein HH (2019) Assessment the norms for agricultural soils in Ghammastown, Iraq. Plant Arch 19:1483–1490
25. OECD (1979) Exposure to radiation from the natural radioactivity in building materials. Report by an NEA group of experts, Paris

26. UNSCEAR (1993) Sources and Effects of Ionizing Radiation. United Nations Scientific Committee on the Effect of Atomic Radiation.
27. Masok FBB, Masiteng PLL, Mavunda RDD et al (2018) Measurement of radioactivity concentration in soil samples around phosphate rock storage facility in Richards Bay, South Africa. J Radiat Res Appl Sci 11:29–36. https://doi.org/10.1016/j.jrras.2017.10.006
28. Majeed KF, Salama E, Elfiki SA, Al-Bakhat YMZ (2021) Natural radioactivity assessment around the petroleum-producing areas of The-Qar province. Iraq Environ Earth Sci 80:64. https://doi.org/10.1007/s12665-020-09316-5
29. Raste PM, Sahoo BK, Bakshi AK et al (2020) A study on natural radioactivity and potential of 222Rn, 220Rn exhalation from Deccan table land of Kolhapur district, Maharashtra, India. J Radioanal Nucl Chem 326:1333–1341. https://doi.org/10.1007/s10967-020-07384-2
30. Najam LA, Younis SA, Kithah FH et al (2015) Natural radioactivity in soil samples in nineveh province and the associated radiation hazards. Int J Phys. https://doi.org/10.12691/ijp-3-3-6
31. Alzubaidi G, Hamid FBS, Abdul Rahman I (2016) Assessment of natural radioactivity levels and radiation hazards in agricultural and virgin soil in the state of Kedah. North of Malaysia Sci World J 2016:6178103. https://doi.org/10.1155/2016/6178103
32. Yang B, Zhou Q, Zhang J et al (2019) Assessment of radioactivity level and associated radiation exposure in topsoil from eastern region of Shangrao Prefecture, China. J Radioanal Nucl Chem 319:297–302. https://doi.org/10.1007/s10967-018-6298-y
33. Boukhenfouf W, Boucenna A (2011) The radioactivity measurements in soils and fertilizers using gamma spectrometry technique. J Environ Radioact. https://doi.org/10.1016/j.jenvrad.2011.01.006
34. Turhan Ş, Gören E, Uğur FA et al (2018) Study of the radioactivity in environmental soil samples from Eastern Anatolia Region of Turkey. Radiochim Acta. https://doi.org/10.1515/ract-2017-2845
35. Fathivand A, Moradi M, Kashian S (2014) Radiological impact of phosphate fertilizers on the agricultural areas in Iran. Radiat Prot Environ 37:2–5. https://doi.org/10.4103/0972-0464.146449
36. Abojassim AA, Rasheed LH (2021) Natural radioactivity of soil in the Baghdad governorate. Environ Earth Sci 80:10. https://doi.org/10.1007/s12665-020-09292-w
37. Hameed PS, Pillai GS, Mathiyarasu R (2014) A study on the impact of phosphate fertilizers on the radioactivity profile of cultivated soils in Srirangam (Tamil Nadu, India). J Rad Res Appl Sci 7(4):463–471
38. Krishnan C, Kumari B, Sivakumar G et al (2014) Evaluation of oral hygiene status and periodontal health in Down's syndrome subjects in comparison with normal healthy individuals. J Indian Acad Dent Spec Res 1:47